

THE MIOCENE ENNS VALLEY BASIN (AUSTRIA) AND THE NORTH ENNS VALLEY FAULT

Melanie KEIL¹ & Franz NEUBAUER

KEYWORDS

Enns Valley Miocene
provenance analysis
tectonic deformation
lateral extrusion
basin inversion
seismicity

Dept. Geography and Geology, University of Salzburg, Hellbrunner Straße 34, A-5020 Salzburg, Austria;

¹ Corresponding author, melanie.keil2@sbg.ac.at

ABSTRACT

The Miocene Enns Valley basin initiated along the ENE-trending Salzach-Enns-Mariazell-Puchberg fault and this fault separates the exhumed Hohe and Niedere Tauern blocks from the Miocene basin fill. Deposits of the Miocene Enns Valley basin occur in a number of dispersed exposures along the northern valley margin and are nearly exclusively derived from the southern Ennstal Quartzphyllite, Wölz Micaschist and Schladming/Bösenstein complexes. We also recognized a very specific, unique contributor, the Hochgrößen serpentinite massif. The Enns Valley basin fill is confined and disrupted along its northern margin by the North Enns Valley fault, a hitherto unidentified fault, which separates the Miocene Enns Valley basin from the Northern Calcareous Alps. The North Enns Valley fault postdates the deposition of the Miocene Enns Valley basin fill and likely extends to the WSW into the Mandling fault and, to the ENE, into the Pyhrn fault. If this interpretation is correct, then a ca. 20 km dextral offset and ca. 1–1.2 km northern block up displacement occurred along this fault, mostly during the Late Miocene/Early Pliocene inversion during E–W shortening as postulated by previous models. Dextral displacement along the North Enns Valley fault could also explain the Weyer Arc, a specific feature within the eastern Northern Calcareous Alps. This arc could be explained by accommodating a dextral displacement at the eastern termination of the North Enns Valley fault by counterclockwise rotation.

Das miozäne Ennstalbecken entwickelte sich entlang der ENE verlaufenden Salzach-Enns-Mariazell-Puchberg Störung. Diese Störungszone trennt die exhumierte Blöcke der Hohen und Niederen Tauern von miozäner Beckenfüllung. Eine Anzahl voneinander getrennter Aufschlüsse entlang des nördlichen Talrandes sind dem Miozän des Ennstales zuzuordnen. Gespeist sind diese beinahe exklusiv von den südlich gelegenen Ennstal Quartzphyllit-, Wölz Micaschist- und Schladming/Bösenstein Komplexen. Ein spezifischer Eintrag an Material stammt aus dem Höchstgrößen Serpentin Massiv. Eine bislang unidentifizierte Störung, die Nord-Ennstal Störung begrenzt das Ennstal-Miozän im nördlichen Randbereich und trennt dieses von den Nördlichen Kalkalpen. Die Nord-Ennstal Störung ist jünger als das miozäne Ennstalbecken und erstreckt sich WSW hin zur Mandlingstörung und ENE zur Pyhrnstörung. Wenn diese Interpretation korrekt ist, dann erfolgten entlang dieser Störung ein dextraler Versatz um ca. 20 km und ein vertikaler Versatz des nördlichen Blocks um ca. 1–1.2 km. Dies geschah im Zuge der Inversion im Spät-Miozän/Früh-Pliozän während einer E–W Verkürzung, wie es frühere Modelle bereits postulierten. Die dextrale Versetzung entlang der Nord-Ennstal Störung könnte auch die Weyerer Bögen erklären, die ein spezifisches Charakteristikum innerhalb der Nördlichen Kalkalpen darstellen. Die bogenförmige Struktur ließe sich daraus erklären, dass sie einen Teil des dextralen Versatzes am Ostende der Nord-Ennstal Störung durch Rotation gegen den Uhrzeigersinn ausgleicht.

1. INTRODUCTION

The Oligocene to Neogene fault pattern of the Eastern Alps has been interpreted to result from lateral extrusion due to indentation of the rigid Southalpine indenter (e. g. Ratschbacher et al., 1989, 1991; Robl and Stüwe, 2005a, b). Most faults are oriented roughly E–W. Among these, the sinistral Salzach-Enns-Mariazell-Puchberg (SEMP) and Mur-Mürz faults stretch along the northern margins of the eastward extruding block, the Periadriatic fault along its southern edge (Neubauer, 1988; Ratschbacher et al., 1989, 1991 and references therein; Fig. 1A). The sinistral faults are often associated with Early Miocene sedimentary basins interpreted as pull-apart and transcurrent basins (Strauss et al., 2001). The orogen-parallel drainage developed preferentially along these basins (Neubauer, 1988; Ratschbacher et al., 1989, 1991; Frisch et al., 2000a, b; Robl et al., 2008a, b).

In spite of the importance, most of these Miocene basins are poorly studied with respect to their structure, provenance of sediments and lithofacies. This is particularly true for the poorly exposed and dispersed remnants of Miocene sedimentary successions along the Enns Valley between Gröbming and Wörschach (Sachsenhofer, 1988 and references therein; Figs. 1, 2). This contribution presents facies, provenance and structure of these basins and some intriguing features never considered before, which challenge previous models. Beside the well known segment of the SEMP fault at the southern edge of the Enns Valley, the various remnants of these Miocene succession are confined to the north against the main body of the Northern Calcareous Alps (NCA) by another major fault, which we term North Enns Valley (NEV) fault and which is an extension of the Mandling fault in the west. It seems that

the SEMP and NEV faults were often confounded in the past (Neubauer, 1988; Ratschbacher et al., 1991; Peresson and Decker, 1997a, b; Wölfler et al., 2011). The vertical throw is more than one kilometer. Furthermore, we demonstrate that a medium-grade metamorphic basement is the principal source of detritus deposited within these Miocene basins. Although adjacent to the Northern Calcareous Alps, hardly any detritus from the NCA was found within these Miocene basin remnants. The dearth of limestone clasts suggests the main uplift stage of the NCA post-dates the deposition of the Miocene basin

remnants (e.g., Sachsenhofer, 1998). This demonstrates that the North Enns Valley fault was not active during deposition of the Miocene sediments, and has significant implications for the sequence of fault activation.

To fill a gap in the knowledge of the Miocene Enns Valley basin the current paper focuses on two topics:

- 1) The small isolated remnants of Miocene clastic rocks between Weyern (Gröbming) and Wörschach, where detailed lithographic and stratigraphic classifications were not available (Fig. 2).

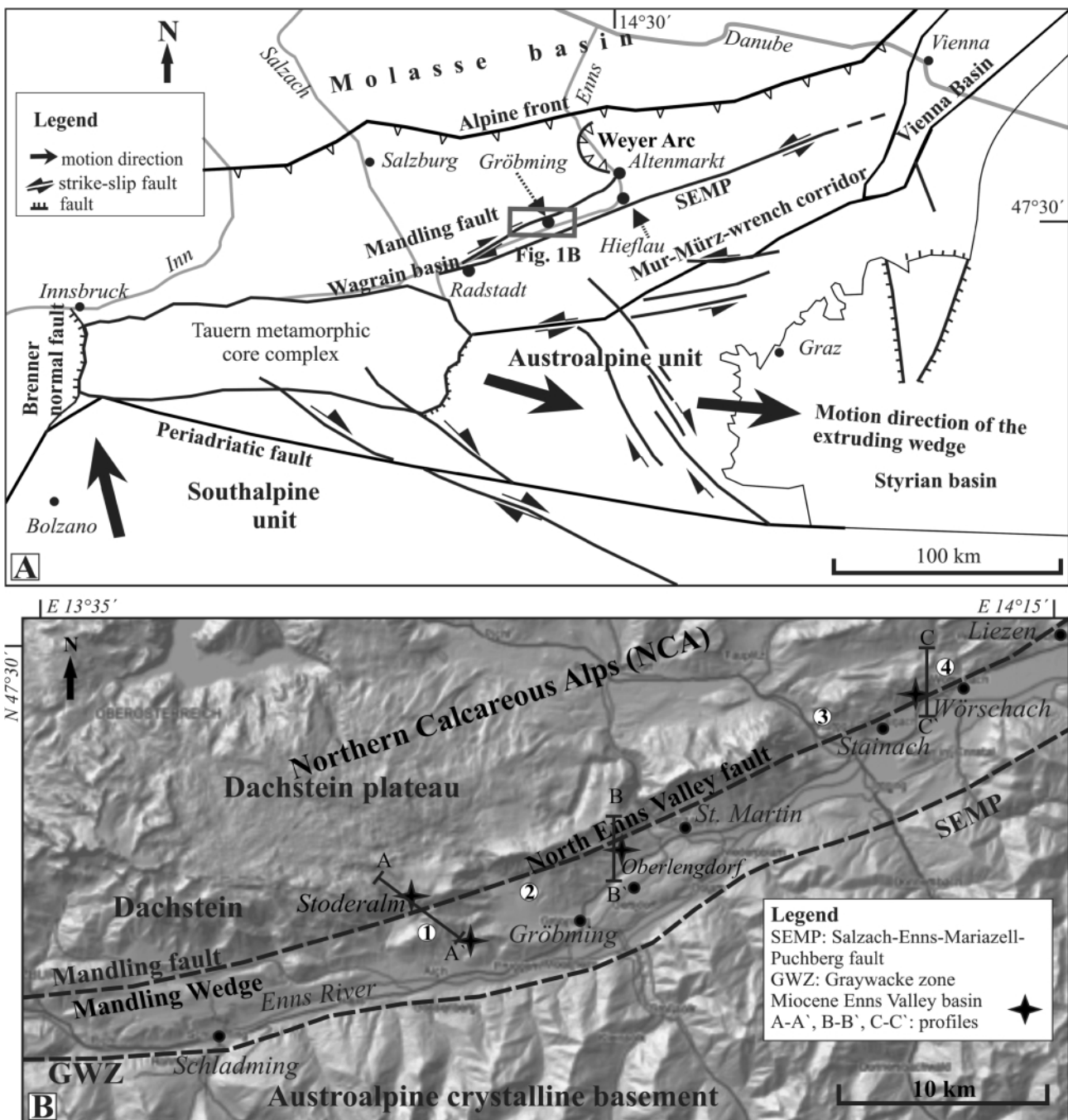


FIGURE 1: A – Simplified tectonic map of the Eastern Alps showing N–S shortening and lateral extrusion (modified from Keil and Neubauer, 2009). B – Digital elevation model as close-up to Figure 1A representing a geological overview and the locations of the principal strike-slip faults. Labelled out-crops indicate the sites where fault and striae data was collected (1 – Road to Stoderzinken, 2 – quarry Gröbming Winkl, 3 Untergrimming, 4 – Wörschach; details to these sites are given in Table 2).

2) The fault zone separating the Northern Calcareous Alps with predominant Dachstein Limestone, Wetterstein Dolomite and Gosau Group Conglomerate from this Miocene clastic succession exposed along the northern slope of the Enns Valley. The goal of the paleostress analysis is to achieve results on kinematics and the dynamics of superimposed tectonic processes also affecting the North Enns Valley basin fill.

2. GEOLOGICAL OVERVIEW

As a result of the collision of the European and Adriatic plates, the morphogenetic evolution of the Eastern Alps started in the Oligocene (from ca. 30 Ma onwards) when conglomeratic fans were deposited in the Molasse zone, derived from the uprising Alps (Frisch et al., 2000a, b; Genser et al., 2007; Robl et al., 2008a, b). The Oligocene and Miocene Molasse deposits resulted from a growing relief along the central axis of the Eastern Alps. Ca. N–S directed plate convergence caused thrusting and crustal thickening during continental collision (Ratschbacher et al., 1989, 1991; Neubauer and Genser, 1990; Neubauer, 1994; Peresson and Decker, 1997a, b; TRANSALP Working Group, 2002). An important feature of eastern sectors of the Northern Calcareous Alps and central sectors of the Eastern Alps is the Salzach-Enns-Mariazell-Puchberg (SEMP) fault striking WSW–ESE over 400 km from the northern Tauern window in the west to the Vienna Basin in the east (e.g. Ratschbacher et al., 1991; Nemes et al., 1995; Linzer et al., 1997, 2002). The SEMP-fault represents the northern margin

of the principal eastward extruding block. According to Frisch et al. (2000), the escaping block east of the Tauern window has largely transtensional border faults with pull-apart basins along its margins.

Lateral extrusion of the Eastern Alps started in the Late Oligocene and accumulated in Early and Middle Miocene times (e.g., Decker et al., 1994; Frisch et al., 2000a). In the northern sectors of the Eastern Alps, numerous mostly orogen-parallel sinistral strike-slip fault-systems were the consequence of indentation and lateral tectonic extrusion (Ratschbacher et al., 1989, 1991; Peresson and Decker, 1997a, b; Frisch et al., 1998, 2000; Wang and Neubauer, 1998; Sachsenhofer, 2001; Wagrreich and Strauss, 2005) (Fig. 1A). Intense Neogene strike-slip tectonics was responsible not only for the eastward extrusion of the Austroalpine upper crust but also for the development of west-east trending fault-controlled valleys (e.g. Paleo-Enns and Paleo-Mur-Mürz) (Dunkl et al., 2005) and fault-controlled basins (e.g. Wagrain, Stoderalm, Hiefalau). Investigations in the westernmost Wagrain sedimentary basin between Altenmarkt and Wagrain demonstrate that the development of the basin is concurrent with the formation of the Salzach-Enns and Mandling faults in Early Miocene times (Wang and Neubauer, 1998; Neubauer, 2007). The Salzach-Enns strike-slip fault as a segment of the SEMP fault trends ENE (Wang and Neubauer, 1998; Ratschbacher et al., 1991) and is supposed to run along the Enns Valley in the study area. The Enns River separates the crystalline basement, particularly the Ennstal Phyllite unit of the Niedere Tauern in the south from the Gray-

SEMP: Salzach-Enns-Mariazell-Puchberg fault
 GWZ: Graywacke zone
 NCA: Northern Calcareous Alps
 NEV: North Enns Valley fault
 MW: Mandling Wedge

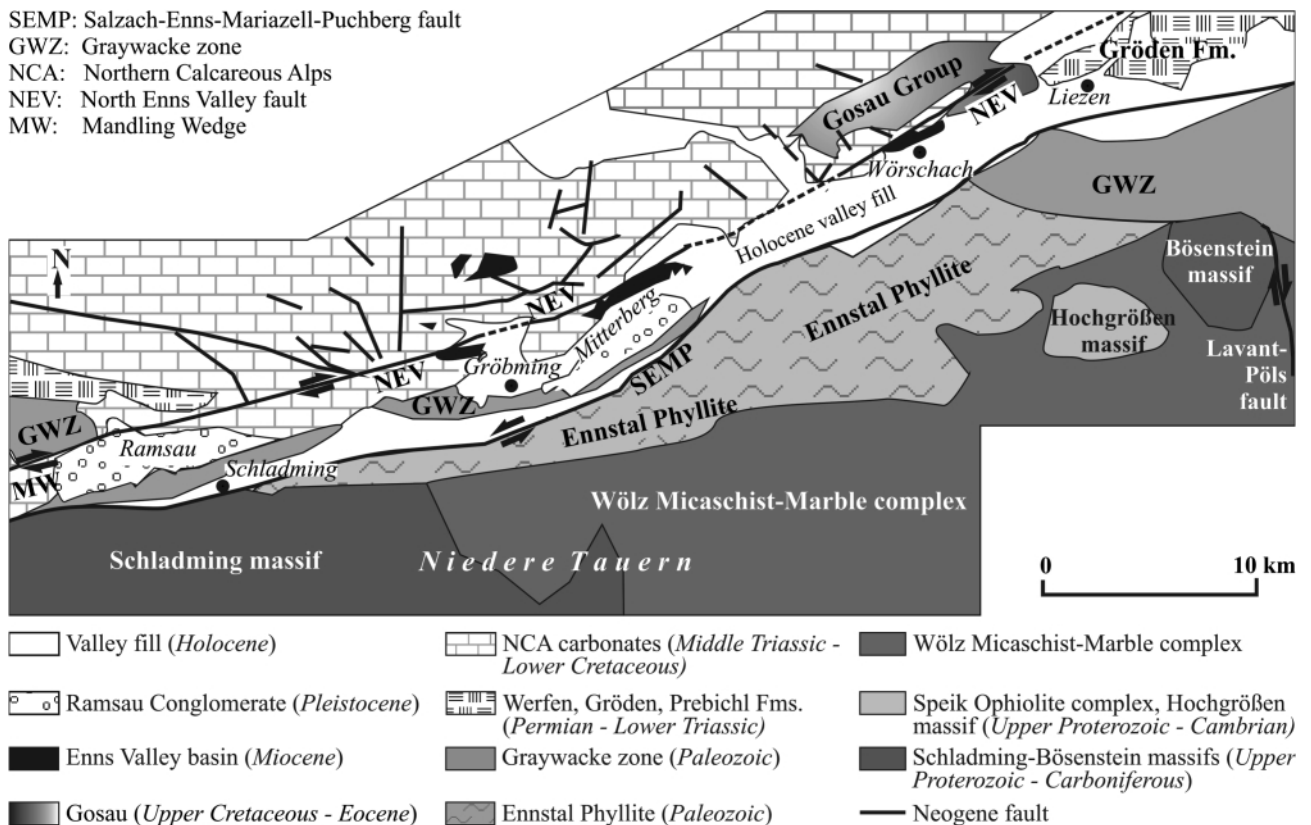


FIGURE 2: Geological overview map of the study area (modified after Reitner et al., 2006).

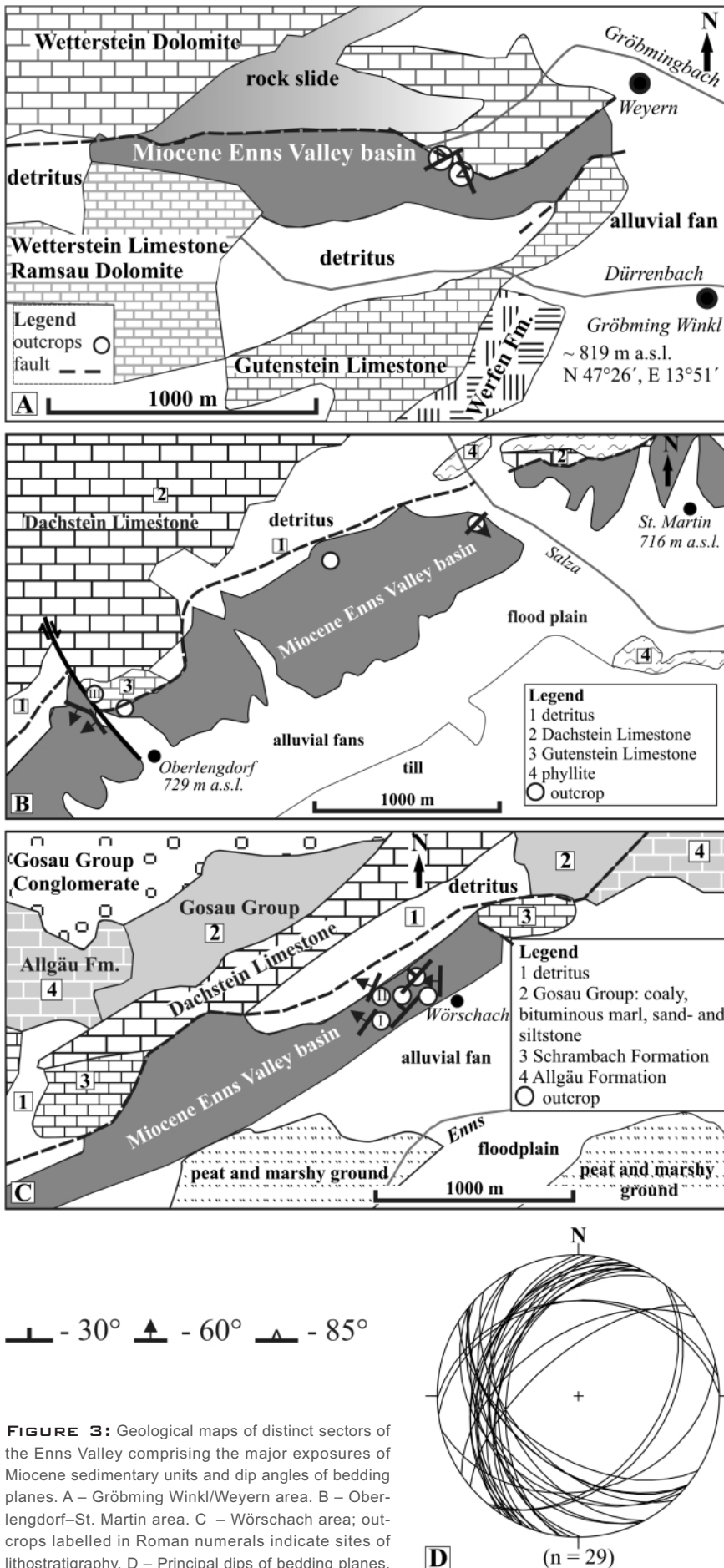


FIGURE 3: Geological maps of distinct sectors of the Enns Valley comprising the major exposures of Miocene sedimentary units and dip angles of bedding planes. A – Gröbming Winkl/Weyern area. B – Oberlengdorf–St. Martin area. C – Wörschach area; outcrops labelled in Roman numerals indicate sites of lithostratigraphy. D – Principal dips of bedding planes.

wacke zone and the Northern Calcareous Alps with the Dachstein plateau in the north (Fig. 1B). In addition, the ENE-trending dextral Mandling fault transects the Graywacke zone in the west, and the Mandling Wedge (Hirschberg, 1965), a unit derived from the Northern Calcareous Alps, is exposed between the Mandling and SEMP faults.

Sandstone and conglomerates – known as the Augenstein Formation – were deposited on a peneplanation surface, which was uplifted later and forms the present-day plateau of the eastern Northern Calcareous Alps (Frisch et al., 2001). The clastic material originated from low-grade metamorphic areas (Hejl, 1997); the absence of higher-grade metamorphic, crystalline material of the Augenstein Formation leads to the assumption that Paleozoic successions covered the Austroalpine crystalline basement (Frisch et al., 2001). Remnants of the above named Miocene basins along the axis of the longitudinal Enns Valley testify the existence of a pre-Pleistocene depression.

Previous concepts on age-dating of the Miocene Enns Valley basin fill included the comparison with the Augenstein Formation.

a) Supposed Oligocene to Miocene clastic rocks, the so-called Augenstein Formation, have been found on the Dachstein plateau (Frisch et al., 2001 and references therein). Although no fossils are known, the age of the Augenstein Formation is discussed by the overall geologic situation as Early Oligocene to earliest Miocene (Frisch et al., 2001). The Augenstein Formation consists of sandstones and conglomerates rich in polycrystalline vein-derived quartz, typical lithologies for the low-grade metamorphic Variscan Paleozoic succession. The authors exclude the Middle Austro-Alpine crystalline basement as a possible source terrain for the basal Augenstein sediments, as no gneiss, amphibolite and coarse-grained marbles have been found. The late Early Miocene period

(~ 20 Ma) is the uppermost limit for the age of the Augenstein Formation, when fault-bounded depressions formed south of the NCA, thus cutting off the sediment supply from the south.

b) Following Tollmann and Kristin-Tollmann (1963) the deposition of the Augenstein Formation was contemporaneous with the Enns Valley Miocene. Their approach is based upon plant fossils, although their stratigraphic significance is uncertain (e. g. Steininger et al., 1989). More recent data of Miocene Valley remnants at Hieflau compared to the Miocene of the Stoderalm and the Augenstein Formation (Wagreich et al., 1997) exclude an Oligocene age and assume a Lower Miocene age (Ottangian/Karpatian).

c) Another approach to date the Enns Valley Miocene is based upon coal rank (Sachsenhofer, 1988, 2001). The comparison of coal rank between the uplifted Miocene of Stoderalm and the lower located Miocene near Wörschach leads to the conclusion that coalification had terminated before the main uplift stage of the NCA. The coalification process, at least in the coal basin near Stoderalm (~ 1700 m a.s.l.), ended in Aquitanian times (~ 20 Ma).

3. STRATIGRAPHIC UNITS

In the following, we describe major tectono-stratigraphic units bordering the Upper Enns Valley from south to north (Fig. 1B). The Schladming and Bösenstein crystalline basement complexes and the Wölz Micaschist complex (parts of Niedere Tauern) are exposed on the southern side of the Enns Valley. The former consist of a polymetamorphic, Variscan and Alpidic basement with medium- to low-grade para- and orthometamorphic rocks (Mandl and Matura, 1987; Hejl, 1997, 1998). The most frequently occurring rocks in the Schladming and Bösenstein basement complex are para- and orthogneiss, migmatite-gneiss, quartz-phyllite, sericite-quartzite, greenschist, and amphibolite. A peculiar unit is the Hochgrößen massif, a serpentinite body, belonging to the Speik complex, a basement ophiolite (Faryad and Hoinkes, 2001). It represents the only serpentinite body in the catchment of the present-day Enns Valley. The Wölz Micaschist complex mainly comprises

garnet micaschists and some marbles, the latter sometimes associated with Variscan pegmatites (Neubauer, 1988 and references therein). The westernmost part, exposed below the Schladming massif, belongs to the Lower Austroalpine units with the Permian to Triassic Alpine Verrucano-type Quartz-phyllite Group and the Lower Triassic Lantschfeld Quartzite at its stratigraphic base (Mandl and Matura, 1987).

North of the Enns Valley, the Graywacke zone comprises phyllites rich in quartz veins, greenschists, gray metasandstones, and rare calcite and dolomite marbles. South of Liezen (Fig. 2), the Graywacke zone turns ESE, and, in this part, also comprises Carboniferous phyllites, marbles, and conglomerates, as well as some Lower Paleozoic calcite marbles.

In the west, the Graywacke zone is unconformably overlain by the Permian to Upper Jurassic succession of the Dachstein block, which is part of the Northern Calcareous Alps (NCA), (Fig. 1B). The succession includes Permian to Lower Triassic siliciclastic formations (Alpine Verrucano and Werfen Formations). A thick Middle to Upper Triassic dolomite and limestone sequence including the Upper Triassic Dachstein Limestone, forms impressive steep slopes. Jurassic formations are rare. The Triassic sediments accompany the Enns Valley to the east, there also comprising overlying Jurassic and even Lower Cretaceous sedimentary units, which are unconformably covered by clastic Gosau Group sediments of Late Cretaceous and rarely Paleogene age.

4. MATERIALS AND METHODS

Basic materials are the topographic maps ÖK 25V, sheet 127 Schladming, sheet 128, Gröbming, sheet 98, Liezen; Geologische Karte Steiermark, 1:200 000, Geologische Karte Oberösterreich, 1:200 000 and digital elevation models (DEM). Fieldwork focused on the remnants of the Miocene Enns Valley basin, and comprised geomorphologic and sedimentologic investigations in regard to correlation with structural data. A provenance analysis of conglomerates and sandstones has been carried out in detail. Slickenside and striation data was collected along adjacent NCA limestone and dolomite outcrops.

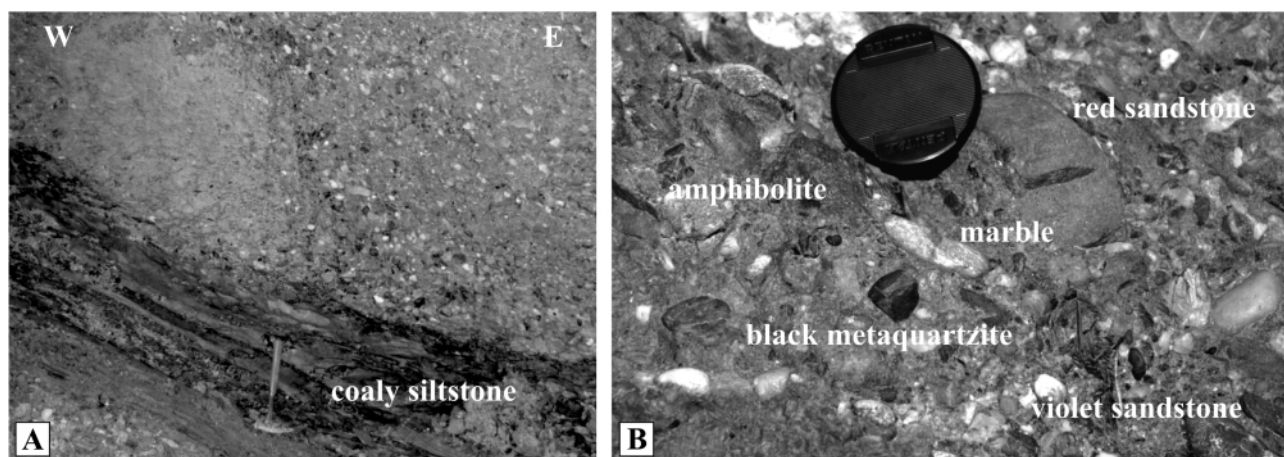


FIGURE 4: Photographs of principal lithofacies units of Miocene sedimentary units: A – Conglomerate with coaly siltstone at the base. B – Typical clasts in the Enns Valley Miocene.

Lithostratigraphic sections

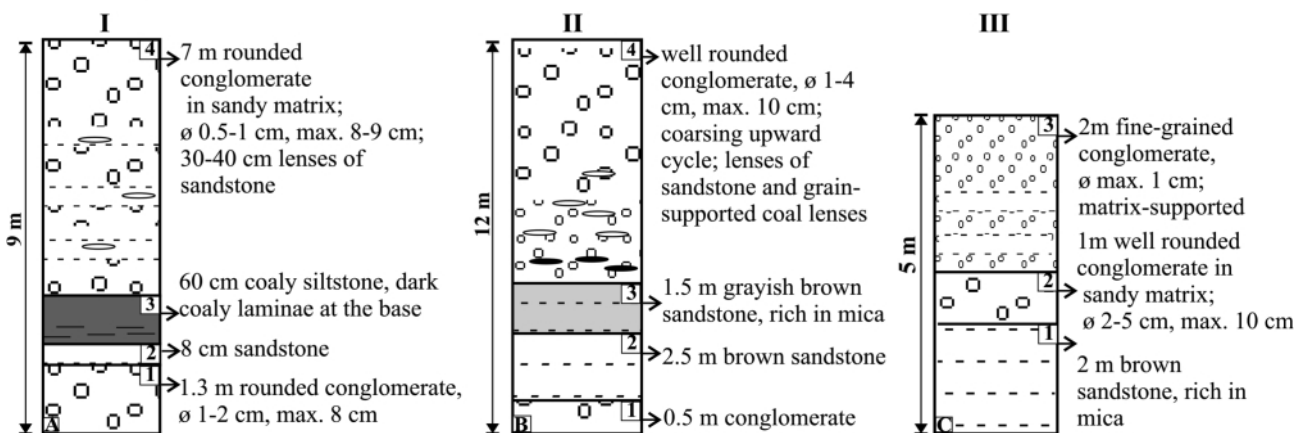


FIGURE 5: Lithostratigraphic sections of Miocene sedimentary units (sites I and II are shown in Fig. 3C, III in Fig. 3B).

Paleostress orientation patterns of faults and slickensides were evaluated by using the TectonicsFP computer programme (Ortner et al., 2002) based on numerical dynamic analysis (NDA) techniques, plot Lambda 1, 2, 3 (Angelier, 1979, 1989, 1994) and the P-T-axes method. The raw data in part contains fault-slip sets with incompatible slip-sense; the TectonicsFP computer programme was used to sort the data and to calculate paleostress tensors (Ortner et al., 2002). For separation to paleostress tensors, only results from outcrops are reported where the number of measurements counts four or more. For details of field work and paleostress analysis, see Tables 1, 2 in the Appendix.

5. MIOCENE ENNS VALLEY BASIN

The longitudinal valley of the Enns River comprises long-known occurrences of lithified Miocene clastic rocks, mostly conglomerate and sandstone (e.g. Winkler-Hermaden, 1951; Tollmann and Kristin-Tollmann, 1963; Weber and Weiss, 1983; Sachsenhofer, 1988, 2001), partly at altitudes of 1650 – 1750 meters, partly in the area and elevation of the northern sectors of the valley-floor. These occurrences include, from west to east, the Miocene of Wagrain and near Radstadt, the Miocene of the Stoderalm, and various Miocene remnants between Gröbming –St. Martin and Wörschach and the Miocene of Hief-lau (for locations see Fig. 1B). We combine all these remnants to the Miocene Enns Valley basin.

5.1 LITHOFACIES SECTIONS OF THE ENNS VALLEY MIOCENE

A simplified geological map depicts the distribution of the Miocene Enns Valley basin and basement surroundings as well as geomorphologic features like recent alluvial fans, peat and marshy grounds and Pleistocene deposits (e.g. Mitterberg) (Fig. 2). Along three sections of the Miocene Enns Valley basin comprehensive investigations have been undertaken. Disadvantages are the limited and vegetated exposures, which complicate lithofacies and structural studies. Figure 3 gives detailed overviews of the investigated realms. In general, the bedding planes show two principal dip directions, e.g. NNW

and SSW (Fig. 3D), so the structure is simple and can be interpreted to result from folding. Upright lithostratigraphic sections can be observed in the three investigated areas.

5.1.1 GRÖBMING-WINKL-WEYERN AREA (FIG. 3A)

The Miocene Enns Valley basin fragments extend over a horizontal distance of about 1.5 km and reach up to 1165 m a.s.l. Short previous descriptions can be found in Petrascheck (1926, 1929) and Cornelius (1945). The accessibility is limited, outcrop conditions are poor and the fragments are highly affected by erosion. Conglomerates dominate the exposures. The few measured bedding planes show two dip directions, NNW and SSW with steep dip angles. Together, they indicate a moderately west-dipping fold.

5.1.2 OBERLENGDORF-ST. MARTIN AM GRIMMING AREA (FIG. 3B)

The relief covered by the Miocene Enns Valley basin fill (mostly sandstones and conglomerates) displays a rather flat topography and altitudes decline from W to E (882 m – 810 m – 687 m a.s.l.). Conglomerates dominate the succession. Their bedding planes dip at an angle < 60° to the SSW. The ca. 0.5 m thick coal seams described by Petrascheck (1926, 1929) have not been found. The easternmost point near the rivulet

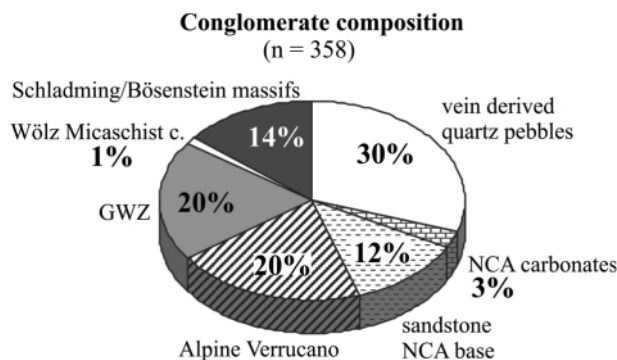


FIGURE 6: Result of the provenance analysis of Miocene conglomerates from the Enns Valley basin fill. GWZ – Graywacke zone; NCA – Northern Calcareous Alps.

Salza comprises Pleistocene conglomerates.

5.1.3 WÖRSCHACH AREA (FIG. 3C)

The Miocene fragments of the Wörschach area are relatively

well exposed. Short previous descriptions can be found in Stur (1853), Häusler (1943), Winkler-Hermaden (1928) and Petrascheck (1926, 1929). The flora originally described by Stur (1853) is unspecific and does not allow a detailed age

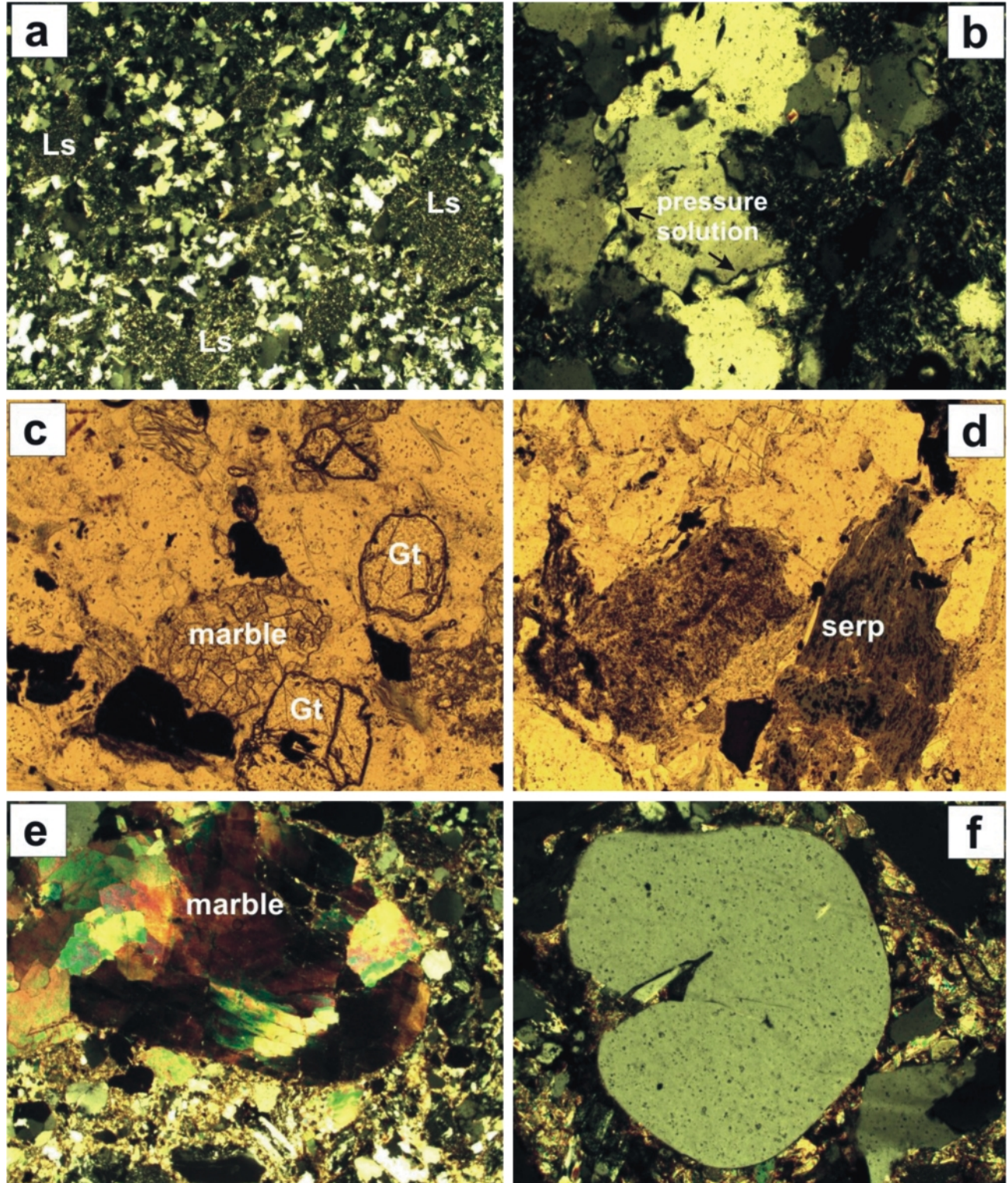


FIGURE 7: Photomicrographs of clasts in sandstones of the Miocene Enns Valley basin. a – Sandstone, very rich in lithic sedimentary components (Ls). b – Sutured grain boundaries (see arrows) due to pressure solution. c – Inclusion-poor garnet (Gt) and marble clasts. d – Serpentinite clast composed of antigorite and fine-grained opaque mineral grains. e – Marble clast with deformed and partly annealed dolomite showing subgrains. f – Phenocrystic quartz likely of volcanic origin, with embayment due to partial resorption. Long edge of a, c, d, e corresponds to 4 mm, b, and f to 1 mm; a, b, e, f: crossed polarizers, c, d: parallel polarizers.

assignment. Winkler-Hermaden (1951) describes a ca. ENE-trending anticline with a gently NNW-dipping northern limb and a subvertical southern limb. At the westernmost part of Wörschach along a new forest road a series of outcrops are accessible, the most impressive one (point I in Figure 3C) is hidden in a trench. Here, we were able to measure various sections (Fig. 5). The sections are dominated by grain-supported conglomerates with well rounded clasts in a sandy matrix. The average grain size of conglomerates varies between 1 and 4 cm, the maximum grain size is ca. 9 – 10 cm. Coarsening upward cycles can be observed (see and compare also Wagreich et al., 1997). Thin coal and sandstone lenses are intercalated within conglomerates. Ca. 60 cm thick coaly siltstone layers are also intercalated within conglomerates (Fig. 4A). Measured sandstone layers are 1.5 – 2 m thick and comprise a carbonatic matrix. The bedding planes dip moderately towards NW and NNW.

5.2 LITHOLOGY OF THE MIOCENE ENNS VALLEY BASIN FILL

Three lithostratigraphic sections of Miocene sedimentary units form the basis for provenance analyses (Fig. 5; locations in Figures 3B, C). The Miocene Enns Valley basin fill consists of fine- to middle-grained conglomerates and variable sandstones, some of which are rich in mica.

5.2.1 CONGLOMERATE

Typical components are vein-derived quartz pebbles, lydite, orthogneiss, variable quartzites, amphibolite, serpentinite, marly/carbonatic phyllite, purple-red sandstone and siltstone of Werfen Formation (Lower Triassic) and subordinate marble and carbonates (Fig. 4B). The pebbles are well rounded and mostly have diameters of up to two centimeters, but pebbles of 8–10 cm diameter also occur. The most striking facts are the dark coaly layers in outcrop I (Fig. 3C) and similar dark coal lenses in outcrop II farther north. Detailed results of the provenance analysis are given in Figure 6 and Table 1. Quartz pebbles are the predominating components in the Miocene sediments (30%), typical for Variscan Paleozoic terrains. Alpine Verrucano (variable quartzites, green sericite schist/phyllite; 20%), lydites and clasts derived from the Graywacke zone (20%) we correlate with lithologies of post-Variscan sequences of the NCA base. 14% of clasts originate from the Schladming/Bösenstein massif, the low proportion of pebbles from the Wölz Micaschist complex is compensated by a high proportion in sandstones. Only three percent of clasts originate from the base of the NCA.

5.2.2 SANDSTONES

The Miocene Enns Valley basin comprises 12% variably colored sandstones (Fig. 6). To establish the source region we examined sandstones from different levels of the Miocene succession of Wörschach, from sections shown in Figure 4. The main aim was to distinguish various sources including the Schladming-Bösenstein gneiss unit, the Wölz Micaschist

unit, the rare Speik complex exposed at Hochgrößen representing the only exposure of ophiolite in the catchment of the Enns Valley, Ennstal Quartzphyllite, the Graywacke zone, and the Northern Calcareous Alps.

Some significant types of grains and of sandstone fabrics are shown in Figure 7. Some samples contain grains with a coating of opaque minerals. The grain sizes vary between 0.06 and 2 mm. The main constituents of the framework fraction >0.06 mm include mainly monocrystalline quartz, subordinate polycrystalline quartz, alkali feldspar, plagioclase, white mica, biotite, chlorite, various carbonates, a wide variety of lithic clasts, then heavy minerals like abundant garnet, rare sphene, rutile, apatite, zircon, tourmaline and opaque minerals (see also Wagreich et al., 1997). In all samples, the contents of lithic sedimentary and meta-sedimentary grains are high, rea-

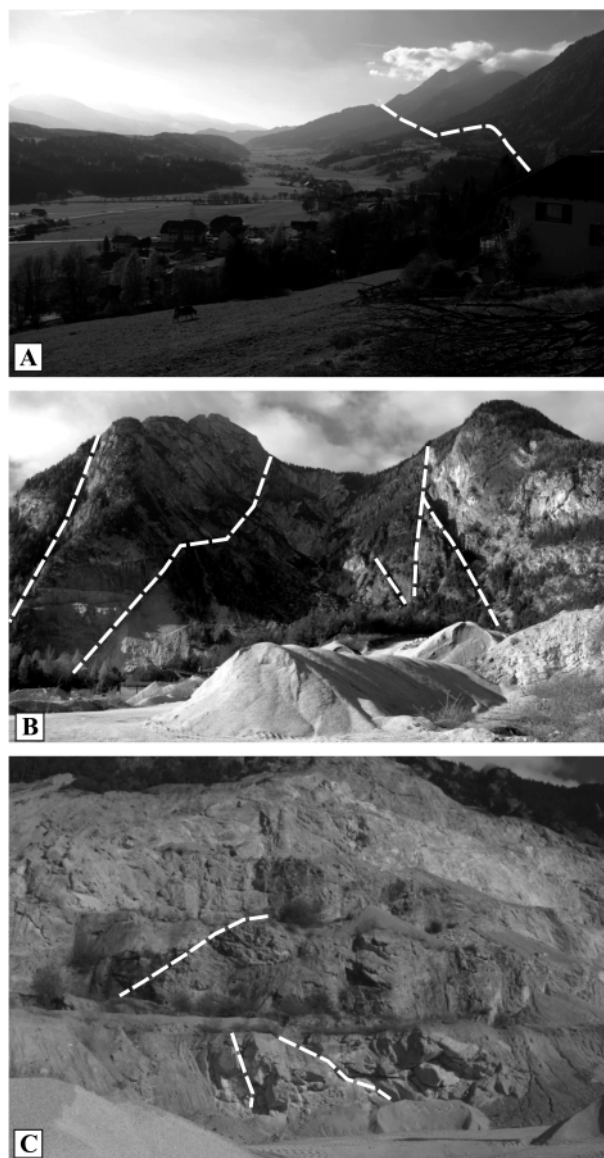


FIGURE 8: A – View along the northern margin of the Enns Valley toward the W, approximate trace of the North Enns Valley fault is shown. B – A series of faults bordering the Miocene Enns Valley basin at Gröbming Winkl–Weyern; view towards west. C – Quarry at Gröbming/Winkl, upper side Dachstein Limestone, bottom Wetterstein Dolomite.

ching up to ca. 40 percent of the framework constituents (Fig. 7a). In many sandstone samples, clasts and matrix are deformed. Pressure solution at quartz-quartz grain contacts is common, and some quartz grains developed a serrated grain boundary (Fig. 7b). This feature was unexpected.

The specific features of some minerals provide detailed evidence for a specific source. Broken garnet grains occur in a size of up to 1.5 mm (Fig. 7c); some are free of any inclusions whereas others include abundant quartz inclusions. In one case, a chloritoid grain was observed. Garnet is a common mineral in the Wölz Micaschist unit. White mica and biotite occur in relatively large grains of up to 0.5 mm typical for micaschist. Biotite grains are mostly brownish, and many include ilmenite exsolutions. In other cases, biotite grains are nearly entirely transformed into chlorite with crystallographically oriented sagenite (rutile) exsolutions. Polycrystalline quartz grains occur in two basic types. Small, often strongly elongated quartz grains with serrated grain boundaries are typical for low-grade metamorphic quartz mylonites. Other polycrystalline quartz grains are very fine-grained and are nearly not recrystallized. Slate, metasiltstone and phyllite clasts are very common and many of them are slightly graphitic or dark-colored due to a mixture of finest opaque mineral grains. Some phyllite clasts show a well preserved crenulation cleavage. Clasts of quartz micaschists are retrogressed as biotite is partly altered to chlorite. In two samples, serpentinite clasts were found comprising antigorite and ore minerals (Fig. 7d). A low proportion of well rounded carbonate clasts, calcite and dolomite marble, occurs in a few samples (Fig. 7e). Roundness often contrasts other clasts (Fig. 7d). Carbonate grains occur as monocrystalline untwinned calcite and dolomite clasts, as well as recrystallized

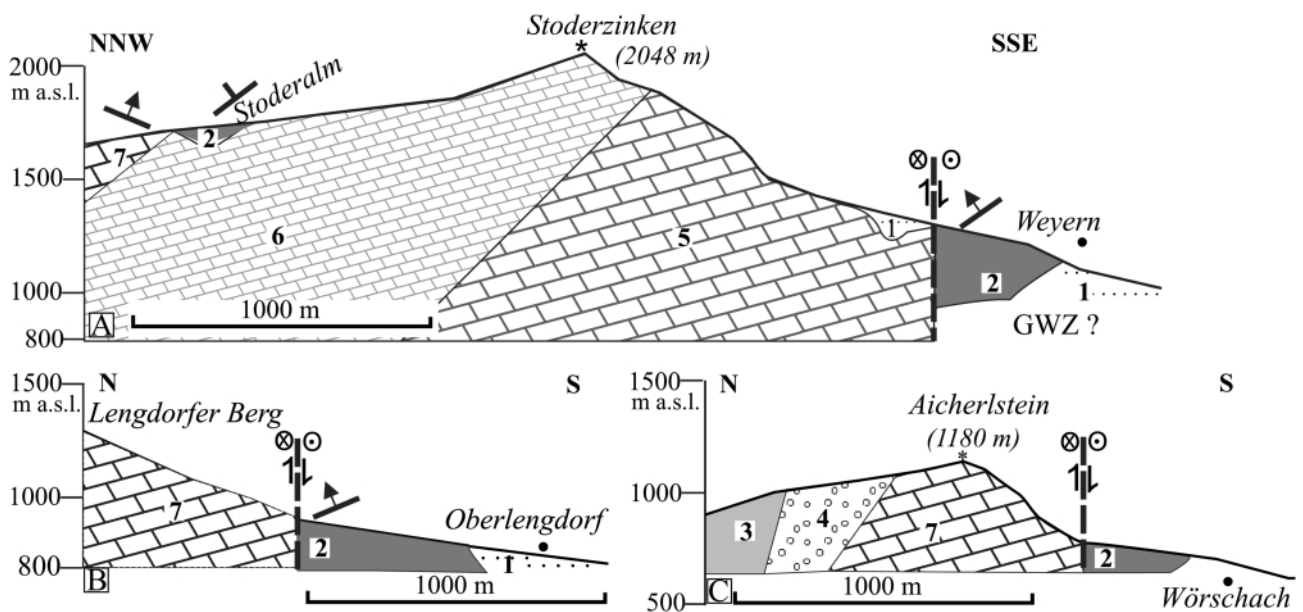
sparitic calcite marble, and rarely as slightly recrystallized micritic limestone. A few metavolcanic and unmetamorphic acidic volcanic clasts were observed. Such minerals include often broken, but still recognizable euhedral monocrystalline quartz with embayments similar to volcanic phenocrysts, which indicate acidic volcanics (Fig. 7f). Metavolcanic clasts are greenschists with chlorite, plagioclase and leucoxene/sphene as main minerals.

The matrix of sandstones comprises low proportions of epimatrix of phyllosilicates derived from slate squeezed between rigid quartz clasts, and some sandstone samples are partly cemented by calcite. The matrix and cement proportion is low (less than 10 percent). In summary, sandstones are, therefore, generally relatively poorly sorted lithic arenites.

We also examined a few siltstone samples, which often contain a low proportion of fine clasts of the sand fraction. These samples are particularly rich in mica, and the proportion of mostly brownish biotite is high.

6. NORTH ENNS VALLEY FAULT

In the westernmost sectors of the ca. ENE-trending Upper Enns Valley, the Mandling fault merges with the SEMP fault (Wang and Neubauer, 1998; see also Reitner et al., 2006), and the Miocene Wagrain basin is exposed to the north of both faults (Fig. 1A, B). In the north, the Mandling fault confines the Mandling Wedge (Fig. 1B). The Mandling Wedge comprises rare lenses of Lower Triassic Werfen Quartzite cut at the base by faults, mainly Middle Triassic Gutenstein Dolomite and Upper Triassic Dachstein Limestone (Hirschberg, 1965; Matura, 1987). Neubauer (2007) assumes a ca. 20 km dextral offset as the Mandling Wedge could represent a strike-slip du-



Legend
 1 detritus, 2 Miocene Enns Valley basin, 3 Gosau (above Base Conglomerate), 4 Gosau Base Conglomerate, 5 Wetterstein Dolomite, 6 Wetterstein Limestone, 7 Dachstein Limestone

FIGURE 9: Simplified structural profiles showing the location of the Enns Valley Miocene near the lower Enns Valley and the North Enns Valley fault. GWZ – Graywacke zone.

plex of the Northern Calcareous Alps displaced from the eastern Dachstein plateau. This also implies a vertical throw of ca. 1 to 1.2 km. New geological maps of the scale 1:200 000 (Braunstingl et al., 2005; Braunstingl and Hejl, 2009; Reitner et al., 2006) already show that the Mandling fault could extend to the east, where it forms, as we defined above, the North Enns Valley fault (Fig. 8A). Several sections (Fig. 9) show these relationships. In some cases, like on the southern slope of the Stoderzinken (Fig. 8B), the NEV fault juxtaposes the Miocene Enns Valley basin fill to steep walls of the southernmost NCA. The southernmost sectors of NCA are transected by many steep faults confining shear lenses with relatively well preserved Middle and Upper Triassic carbonates (Fig. 8C).

7. STRUCTURE OF THE MIOCENE ENNS VALLEY BASIN

Three profiles across the Miocene Enns and its boundary

units (Fig. 9, locations in Fig. 1B) present a unique situation. The previously described anticline of the Wörschach area has not been found due to the relatively poor exposure. However, the NNW dip indicates a post-depositional northwestern tilting of strata towards the NEV fault.

The Ennstal Valley basin follows a succession of limestone and dolomite from N to S, and is generally bordered by a steep to subvertical normal fault in the north (Fig. 9). This major fault suggests, therefore, Neogene activity, apart from the SEMP, postdating deposition of the Enns Valley basin fill as nearly no NCA clasts occur within the basin fill.

7.1 PALEOSTRESS IN THE BASEMENT

Detailed fault-slip data and paleostress assessment from the SEMP fault were mainly published from the segment north of the Tauern window (Wang and Neubauer, 1998; Frost et al., 2011), Schladming area (Keil and Neubauer, 2011) and from

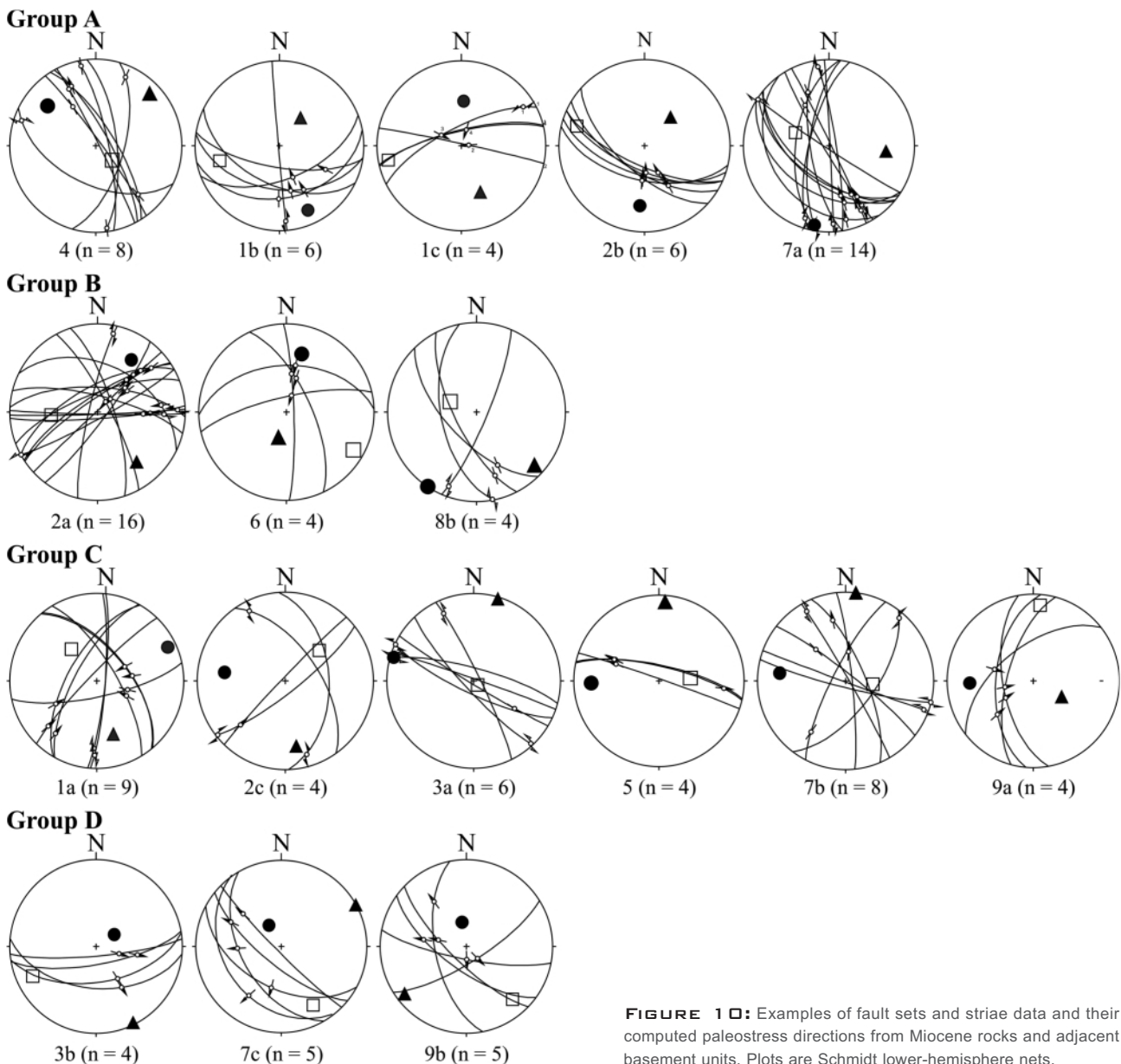


FIGURE 10: Examples of fault sets and striae data and their computed paleostress directions from Miocene rocks and adjacent basement units. Plots are Schmidt lower-hemisphere nets.

easternmost sectors of the Northern Calcareous Alps (Nemes et al., 1995). Further details are available for the Northern Calcareous Alps (Linzer et al., 1997; Peresson and Decker, 1997a, b; Wagreich et al., 1997). From the study area north of the Enns Valley, no data was published so far. Here, we present data collected from the Miocene sediments as well as from adjacent NCA units. A list of stations together with geographic coordinates and lithologic descriptions is given in Table 2.

To build up a paleostress stratigraphy we follow the analysis of Peresson (1992), Peresson and Decker (1997a, b) and Linzer et al. (1997) from the adjacent Northern Calcareous Alps and that of Wang and Neubauer (1998) from the SEMP fault adjacent in the west. The results of paleostress analysis are displayed in Figure 10.

Fault plane analyses enable the establishment of a relative chronology of four deformational phases. Hereby, we largely followed the subdivisions and age assignments set up by Peresson and Decker (1997a, b) as insufficient evidence for timing was found in the working area itself.

- Group A defines an N–S compressional regime (early Middle Miocene), dextral NNW-trending strike-slip- and thrust faults dominate. In one case, we found NW–SE strike-slip compression.
- Group B comprises NE–SW strike-slip compression (Middle Miocene), NE-trending strike-slip faults dominate.
- Group C comprises NW to N trending sinistral strike-slip faults and steep NE-trending dextral strike-slip faults. Together these faults indicate ca. E–W compression (Late Miocene/Early Pliocene according to Peresson and Decker, 1997a, b).

- Group D defines NNE–SSW (NE–SW) extension (Late to post-Miocene) by variably oriented normal faults.

7.2 RECENT SEISMICITY

The far-field stress field by indentation of the Adria/Southalpine indenter is considered to control already described local paleostress orientations of the Austroalpine and Penninic units of the Eastern Alps along western (e.g. Wang and Neubauer, 1998; Frost et al., 2011) and easternmost sectors of the Salzach-Enns-Puchberg-Mariazell fault (Nemes et al., 1995). Further details are available for the Northern Calcareous Alps (Linzer et al., 1997; Peresson and Decker, 1997a, b), and only limited data is available for active tectonic structures (see below). Previous assessments on seismicity were conducted by Reinecker and Lenhardt (1999) and Keil and Neubauer (2011). However, none of these studies put possible relationships of seismicity to the Mandling and NEV faults.

Present-day seismic activity is low along the SEMP south of the valley (Reinecker, 2000) and high further north of it (see below) (Fig. 11). A whole row of recent earthquakes reaching magnitudes of >4 occur in line with the Mandling fault and its extension in the North Enns Valley fault (Fig. 11). In the study area, seismic activities have been recorded though at low magnitudes. Within the polygon grid Ennstal (47.30 – 13.20; 47.30 – 14.20; 47.60 – 14.20; 47.60 – 13.20) 137 seismic events have been recorded since 1897 (Rieder, pers. comm. 2005; Meurers, pers. comm. 2010); local magnitudes are between 0.7 and 4.1 (Fig. 11); hypocenters are located at a depth between 6 and 8 km (Lenhardt et al., 2007). Interestingly, many major events are located at or close to the Mandling and NEV faults. Con-

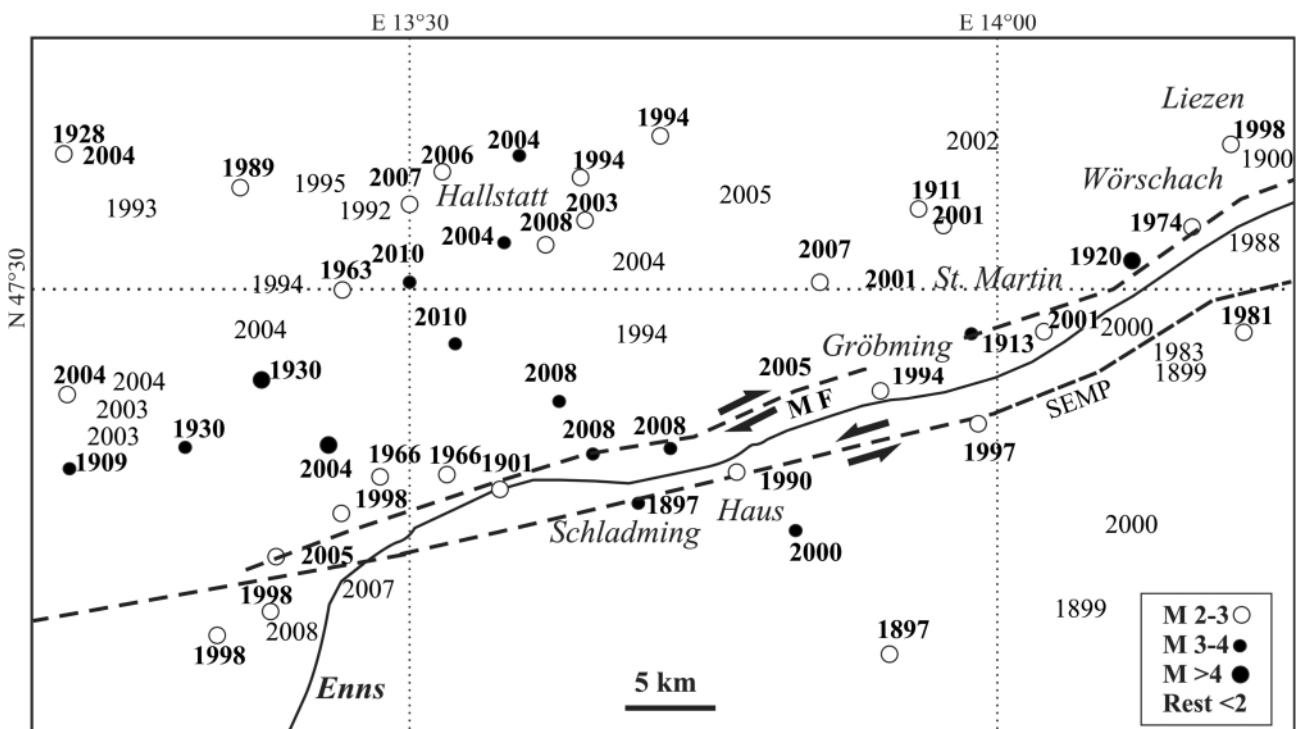


FIGURE 11: Distribution of seismic events in the extended study area (M = magnitude, MF = Mandling fault; from Rieder, pers. comm., 2005 and Meurers, pers. comm., 2010).

sequently, these seismic events indicate recent activity along the North Enns Valley fault.

8. DISCUSSION AND CONCLUSION

It appears that the Miocene Enns Valley basin is still being under-investigated, as is demonstrated by our recent findings on field geology and structures. In the following, we discuss aspects of the evolution of the Miocene sedimentary units of Enns Valley basin fill. We first discuss basin-forming mechanisms of the SEMP fault and basin destruction by the activity of the North Enns Valley fault. Then, we discuss the significance of the faults, particularly of the North Enns Valley fault. Finally, we integrate all data in an overall new model of the Upper Enns Valley, which may serve as a model for similar orogen-parallel fault-controlled valleys in the Eastern Alps and trigger future, more detailed studies on other faults.

8.1 PROVENANCE

The clasts in conglomerates and sandstones of the Miocene Enns Valley basin allow detailed insights into possible sources. First, nearly no un-metamorphic carbonates (limestone, dolomite) are preserved but exclusively marbles. This fact excludes the Middle Triassic to Cretaceous carbonates of the Northern Calcareous Alps as a significant source of the Miocene Enns Valley basin succession and argues for an exclusive source in the south of the present-day Enns Valley. Large white mica and brownish, Ti-rich biotite flakes, and garnet in sandstones indicate the Wölz Micaschist unit as a major contributor. Large monocrystalline calcite and dolomite grains could derive from marble layers included in the Wölz Micaschist unit and or from the Graywacke zone. The serpentinite clasts have a unique source, likely the Hochgrößen serpentinite body, the only serpentinite body in the catchment of the Enns Valley. Phyllite and the rare greenschist is representative for both the Ennstal Quartzphyllite and the Noric unit of the Graywacke zone. Calcitic marbles, slate and metasiltstones could derive from the Noric unit of the Graywacke zone. Graphitic admixtures are particularly abundant in the Veitschnappe, which is a substantial part of the Graywacke zone. All these

sources are exposed to the south of the present-day location of the Miocene Enns Valley basin.

Finally, the acidic volcanic clasts including quartz phenocrysts and acidic microcrystalline matrix point to a stage of acidic tuffs often found in the Styrian basin but also in the Wagrain basin along the SEMP fault (own unpublished observation). The components of the conglomerate are in part different from the Augenstein Formation as reported by Frisch et al. (2001) as they comprise orthogneiss, amphibolite, serpentinite, and marbles, although the vein quartz-dominated inventory of the Augenstein Formation is more mature indicating a longer transport and a higher compositional maturity than the composition of the Miocene Enns Valley basin conglomerates. A similar trend with immature conglomerates at the base and quartz conglomerates in upper portions of the section has been

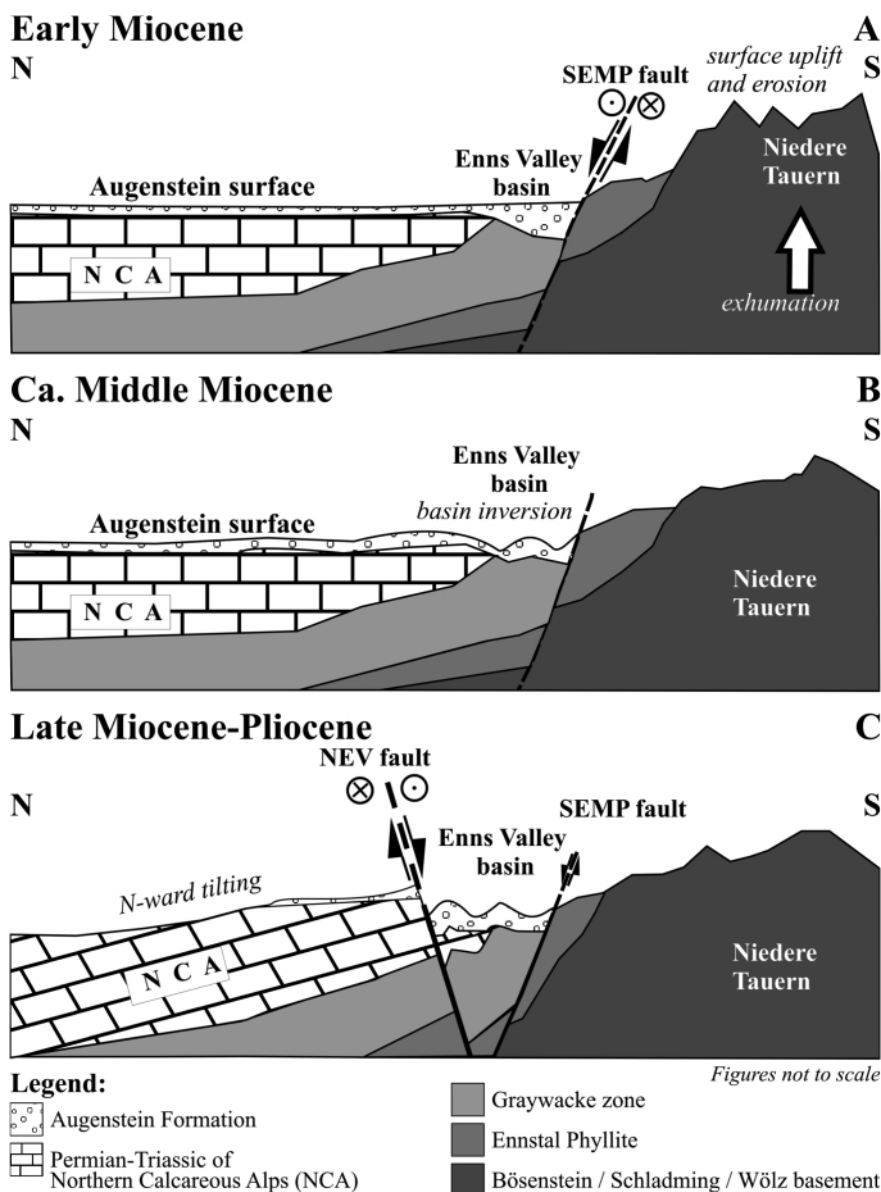


FIGURE 12: Tectonic models for the evolution of the Miocene Enns Valley basin in three steps (A – C) in a sectional view. A – Early Miocene activation of the SEMP, creation of a pronounced topography. B – Basin inversion by ca. N-S to NNW-SSE shortening (present-day coordinates). C – Formation of the North Enns Valley fault by E-W compression.

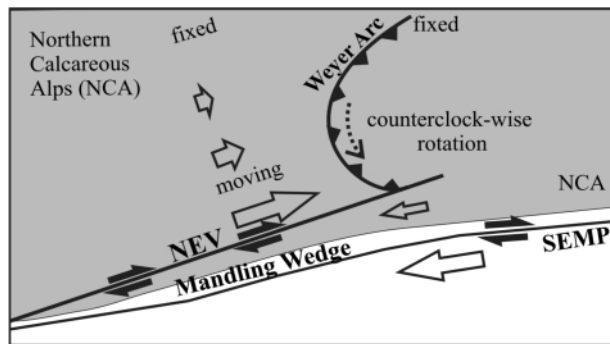


FIGURE 13: Tentative model of formation of the Weyer Arc due to accommodation of dextral slip along the NEV fault resulting in counter-clockwise rotation of the units exposed in the Weyer Arc. Plan view.

found in the Wagrain basin fill (own unpublished observations).

8.2 BASIN FORMING MECHANISM

Our new observations indicate a fluvial-lacustrine depositional environment, which is dominated by conglomerates and remnants of shallow lakes, where mica-rich siltstones were accumulated. Similar fillings of nearby intramontane basins have been described in Strauss et al. (2001) and Wagreeich and Strauss (2005). The conglomerates lack in detritus from the NCA, their coarsening upward cycle suggests a succession of progradation of alluvial fans and fan-deltas. According to Wagreeich et al. (1997) the clastic sediments with coal lenses indicate a raise of the groundwater level related to an Early Miocene transgression.

The exact age of the Miocene Enns Valley fill is uncertain. The Augenstein Formation was interpreted to have been deposited in Late Oligocene to Early Miocene times (Frisch et al., 2001) and needed a source to the south of the SEMP fault. Beside discussed arguments, we note that red paleosoils at the stratigraphic base are known in one Augenstein section (Stoderzinken: Kuhlemann et al., 2008) and at the base of the Miocene Ennstal basin fill (Hieflau: Wagreeich et al., 1997; Wagrain: Neubauer, 2007). These paleosoils are typical for a subtropical climate and could be used tentatively as a correlative stratigraphic horizon suggesting a similar age for both the Augenstein Formation and the Miocene Enns Valley basin fill. We interpret, consequently, both formations as largely contemporaneous. We explain the more immature composition of the Ennstal basin fill as result of a more local source, which developed finally to mature quartz conglomerates (Wagrain basin).

The activation of the SEMP led to a reorientation of the radial drainage pattern to orogen-parallel drainage and stopped the material supply from the Austroalpine basement in Early/Middle Miocene times. Uprising Alps and the activation of a new fault system – the North Enns Valley fault – separated the Miocene Enns Valley basin from the Augenstein Formation. Uplift likely occurred in pulses, interrupted by periods of tectonic dormancy. The Miocene Enns Valley basin north of the Enns River formed a coherent relief with southern realms. Sediment transport from the S/SE was stopped at the new fault system, which confines the Miocene deposits.

From a geomorphologic point of view, Pleistocene glaciation and deglaciation created deep incising rivers and trenches and disrupted the surface (Keil and Neubauer, 2009), thus forming the present-day isolated Miocene basin remnants.

8.3 STRUCTURAL EVOLUTION

In the following, we propose tectonic models for the Neogene evolution of the Enns Valley. The formation of the Miocene Enns Valley basin was likely associated with the activation of the SEMP fault, the formation of a relief within sinistral trans-tensional conditions (Fig. 12A). The Enns Valley basin fills show deformation and folds with ca. W respectively WSW-trending fold axes. These folds imply ca. N-S to SSE-NNW shortening and this is consistent with paleostress tensor A, which must therefore be post-depositional to the Enns Valley basin fill (Fig. 12B). This event may also be responsible for the termination of sedimentation, which was likely associated with a decrease in relief. Similar folds due to N-S shortening were also reported in other Miocene basins in the Eastern Alps, e.g. Leoben, Waldheimat and Fohnsdorf (Petrascheck, 1926, 1929; Neubauer et al., 2000; Sachsenhofer et al., 2000; Strauss et al., 2001; Neubauer and Unzog, 2003). The orientation of slickensides and striae of the Miocene Enns Valley remnants and adjacent units record four different stress stages. Later, at ca. the Late Miocene/Pliocene boundary, the NEV fault was activated and dextral compressional slip occurred along this fault. If this interpretation is correct, then a ca. 20 km dextral offset and ca. 1 – 1.2 km north block up displacement occurred along this fault mostly during the Late Miocene/Early Pliocene inversion as postulated by previous large-scale models of Peresson and Decker (1997a, b) (Fig. 12C). Faults and slickensides of paleostress tensor group C support this interpretation.

Dextral displacement along the NEV and its extension into the Pyhrn fault could also explain the Weyer Arc, a specific feature within eastern Northern Calcareous Alps where the general E-W-strike bends into a N-S direction. The formation of the arcuate structure was initiated along a NE-trending dextral strike-slip fault, and is transected by the Weyer fault (Linzer et al., 2002). The western region of the Weyer Arc is dominated by N-trending normal faults (Decker et al., 1994). The arcuate structure could be explained by partly accommodating dextral displacement at the eastern termination of the NEV fault by counter-clockwise rotation (Fig. 13).

In general, the deformation of the Miocene Enns Valley remnants and the adjacent units of the northern Eastern Alps are characterized by northward thrusting, folding and strike-slip faults due to overall N–S shortening and its overprint by E–W shortening. This underlines the assumption that the North Enns Valley fault is an extension of the Mandling fault, and that it represents a younger system than the SEMP fault.

ACKNOWLEDGEMENTS

The manuscript benefited substantially from the detailed and constructive reviews by Michael Wagreeich, Kurt Stüwe and

Andreas Wöfler. We acknowledge the polishing of the English of the initial version by Isabella Merschdorf.

REFERENCES

- Angelier, J. and Méchler, P., 1977. Sur une methode de recherche des contraintes principales egalement utilisable en tectonique et en seismologie: la methode de dièdres droits. *Bulletin de Societe Geologie de France*, 19, 1309–1318.
- Angelier, J., 1979. Determination of the mean principal directions of stresses for a given fault population. *Tectonophysics* 56 T17–T26.
- Angelier, J., 1989. From orientation to magnitudes in paleo-stress determination using fault slip data. *Journal of Structural Geology*, 11, 37–50.
- Angelier, J., 1994. Fault slip analysis and paleostress reconstruction. In: Hancock, P. (Ed.): *Continental deformation*, p. 53 – 99, Oxford.
- Armijo, R., Carey, E. and Cisternas, A., 1982. The inverse problem in microtectonics and the separation of tectonic phases. *Tectonophysics*, 82, 145–160.
- Braunstingl, R., Hejl, E. and Pestal, G., 2005. *Geologie der österreichischen Bundesländer – Salzburg*. Geologische Karte M 1:200 000. Geologische Bundesanstalt, Wien.
- Braunstingl, R. and Hejl, E., 2009. *Geologie der österreichischen Bundesländer – Salzburg*. Erläuterung zur Geologische Karte M 1:200 000. Geologische Bundesanstalt, Wien.
- Cornelius, H. P., 1945. Zur Schichtfolge und Tektonik des Kammspitz-Grimmingzuges. *Berichte der Reichsanstalt für Bodenforschung Wien*, 1944, 5/8, 127–138.
- Decker, K., Peresson, H. and Faupl, P., 1994. Die miozäne Tektonik der östlichen Kalkalpen: Kinematik, Paläospannungen und Deformationsaufteilung während der „lateralen Extrusion“ der Zentralalpen. *Jahrbuch der Geologischen Bundesanstalt*, 137, 5–18.
- Digitaler Atlas Steiermark, 2010. <http://www.gis.steiermark.at> (accessed on 16-06-2010, 22-06-2010, 20-11-2010, 09-12-2010, 01-02-2011).
- Dunkl, I., Kuhlemann, J., Reinecker, J. and Frisch, B., 2005. Cenozoic relief evolution of the eastern Alps – constraints from Apatite fission track age-Provenance of Neogene intramontane sediments. *Austrian Journal of Earth Sciences*, 98, 92–105.
- Faryad, S.W. and Hoinkes, G., 2001. Alpine chloritoid and garnet from the Hochgrößen massif (speik complex, Eastern Alps). *Mitteilungen der Österreichischen Mineralogischen Gesellschaft*, 146, 387-396.
- Frisch, W., Kuhlemann, J., Dunkl, I. and Brügel, A., 1998. Palinspastic reconstruction and topographic evolution of the Eastern Alps during late Tertiary tectonic extrusion. *Tectonophysics*, 297, 1–15.
- Frisch, W., Székely, B. and Kuhlemann, J., 2000a. Geomorphological evolution of the Eastern Alps in response to Miocene tectonics. *Zeitschrift für Geomorphologie*, 44, 103–138.
- Frisch, W., Dunkl, I. and Kuhlemann, J., 2000b. Post-collisional orogen-parallel large-scale extension in the Eastern Alps. *Tectonophysics*, 327, 239–265.
- Frisch, W., Kuhlemann, J., Dunkl, I. and Székely, B., 2001. The Dachstein paleosurface and the Augenstein Formation in the Northern Calcareous Alps – a mosaic stone in the geomorphological evolution of the Eastern Alps. *International Journal of Earth Sciences*, 90, 500–518.
- Frost, E., Dolan, J., Ratschbacher, L., Hacker, B. and Seward, G., 2011. Direct observation of fault zone structure at the brittle-ductile transition along the Salzach-Ennstal-Mariazell-Puchberg fault system, Austrian Alps. *Journal of Geophysical Research*, 116, B02411, doi:10.1029/2010JB007719.
- Gamond, J.F., 1983. Displacement features associated with fault zones: a comparison between observed and experimental models. *Journal of Structural Geology*, 5, 33–45.
- Gamond, J.F., 1987. Bridge structures as sense of displacement in brittle fault zones. *Journal of Structural Geology*, 9, 609–620.
- Genser J., Sierd A.P.L., Cloetingh S. and Neubauer F., 2007. Late orogenic rebound and oblique Alpine convergence: new constraints from subsidence analysis of the Austrian Molasse basin. *Globaland Planetary Change*, 58, 214–223.
- Häusler, H., 1943. Zur Tektonik des Grimming. *Berichte der Reichsanstalt für Bodenforschung*, 5, 19–53.
- Hejl, E., 1997. ‘Cold spots’ during the Cenozoic evolution of the Eastern Alps: thermochronological interpretation of apatite fission-track data. *Tectonophysics* 272, 159–173.
- Hejl, E., 1998. Über die känozoische Abkühlung und Denudation der Zentralalpen östlich der Hohen Tauern – eine Apatit-Spaltspurenanalyse. *Mitteilungen der Österreichischen Geologischen Gesellschaft* 89, 179–199.
- Hirschberg, K.J., 1965. *Die Geologie des Mandlingzuges (Oberes Ennstal, Österreich)*. Doktorat Thesis University of Marburg/Lahn, 110 pp.
- Keil, M. and Neubauer, F., 2009. Initiation and development of a fault-controlled, orogen-parallel overdeepened valley: the Upper Enns Valley, Austria. *Austrian Journal of Earth Sciences*, 102/1, 80–90.

- Keil, M. and Neubauer, F., 2011. Neotectonics, drainage pattern and geomorphology of the orogen-parallel Upper Enns Valley, Eastern Alps. *Geologica Carpathica*, 62 (in press).
- Kuhlemann, J., Taubald, H., Vennemann, T., Dunkl, I. and Frisch, W., 2008. Clay mineral and geochemical composition of Cenozoic paleosol in the Eastern Alps (Austria). *Austrian Journal of Earth Sciences*, 101, 60-69.
- Lenhardt, W.A., Freudenthaler, C., Lippitsch, R. and Fiegweil, E., 2007. Focal-depth distribution in the Austrian Eastern Alps based on macroseismic data. *Austrian Journal of Earth Sciences*, 100, 66–79.
- Linzer, H.G., Moser, F., Nemes, F., Ratschbacher, L. and Sperner, B., 1997. Build-up and dismembering of the eastern Northern Calcareous Alps. *Tectonophysics*, 272, 97–124.
- Linzer, H.G., Decker, K., Peresson, H., Dell’Mour, R. and Frisch, W., 2002. Balancing lateral orogenic float of the Eastern Alps. *Tectonophysics*, 354, 211–237.
- Matura A., 1987. Schladminger Kristallinkomplex. *Geologische Bundesanstalt Wien, Blatt 127 Schladming*, 13–21.
- Mandl, G.W. and Matura, A., 1987. Geographisch-geologische Übersicht. Tagungsband der Arbeitstagung der geologischen Bundesanstalt 1987, Blatt 127 Schladming, 5–12.
- Marret, R. and Almendinger, R.W., 1990. Kinematic analysis of fault slip data. *Journal of Structural Geology*, 12, 596–612.
- Nemes, F., Pavlik, W. and Moser M., 1995. Geologie und Tektonik im Salztal (Steiermark) – Kinematik und Paläospannungen entlang des Ennstal-Mariazell-Blattverschiebungssystems in den Nördlichen Kalkalpen. *Jahrbuch der Geologischen Bundesanstalt*, 138, 349–367.
- Neubauer, F., 1988. Bau und Entwicklungsgeschichte des Rennfeld-Mugel- und des Gleinalmkristallins (Ostalpen). *Abh. Geologische Bundesanstalt*, 42, 1–137.
- Neubauer, F. and Genser, J., 1990. Architektur und Kinematik der östlichen Zentralalpen – eine Übersicht. *Mitteilungen des naturwissenschaftlichen Vereins für Steiermark*, 120 (METZ-Festschrift), 203–219.
- Neubauer, F., 1994. Kontinentkollision in den Ostalpen. *Geowissenschaften*, 12, 136–140.
- Neubauer, F., Fritz, H., Genser, J., Kurz, W., Nemes, F., Wallbrecher, E., Wang, X. and Willingshofer, E., 2000. Structural evolution within an extruding wedge: model and application to the Alpine-Pannonian system. In: Lehner, F.K. & Urai, J.L. (eds.): *Aspects of Tectonic Faulting (Festschrift in Honour of Georg Mandl)*. Springer-Verlag, Berlin – Heidelberg – New York, pp. 141–153.
- Neubauer, F. and Unzog, W., 2003. Halfgraben formation within an extruding wedge: the Neogene Waldheimat basin in the Eastern Alps. *Neues Jahrbuch für Geologie und Paläontologie Abhandlungen*, 230, 133–154.
- Neubauer, F., 2007. Formation of an intra-orogenic transtensional basin: the Neogene Wagrain basin in the Eastern Alps. 8th Workshop on Alpine Geological Studies (Davos / Switzerland, October 10–12, 2007) Abstract Volume, p. 54.
- Ortner, H., Reiter, F. and Acs, P., 2002. Easy handling of tectonic data: the programs Tectonics VP for Mac and Tectonics FP for Windows. *Computer and Geosciences*, 28, 1193–1200.
- Peresson, H., 1992. Computer aided kinematic analysis of fault sets. *Mitteilungen der Gesellschaft der Geologie- und Bergbaustudenten in Wien*, 38, 107–119.
- Peresson, H. and Decker, K., 1997a. Far-field effects of Late Miocene subduction in the Eastern Carpathians: E–W compression and inversion of structures in the Alpine–Carpathian–Pannonian region. *Tectonics*, 16, 38–56.
- Peresson, H. and Decker, K., 1997b. The Tertiary dynamics of the northern Eastern Alps (Austria): changing paleostress in a collisional plate boundary. *Tectonophysics*, 272, 125–157.
- Petit, J.P., 1987. Criteria for the sense of movement on fault surfaces in brittle rocks. *Journal of Structural Geology*, 9, 597–608.
- Petrascheck, W., 1926, 1929. *Kohlengologie der österreichischen Teilstaaten*. 484 p., Kottowitzer Verlag, Katowice, pp. 1–272.
- Ratschbacher, L., Frisch, W., Neubauer, F., Schmid, S.M. and Neugebauer, J., 1989. Extension in compressional orogenic belts: the Eastern Alps. *Geology*, 17, 404–407.
- Ratschbacher, L., Frisch, W., Linzer, G. and Merle, O., 1991. Lateral extrusion in the Eastern Alps, part 2: Structural analysis. *Tectonics*, 10, 257–271.
- Reinecker, J. and Lenhardt, W.A., 1999. Present-day stress field and deformation in eastern Austria. *International Journal of Earth Sciences*, 88, 532–550.
- Reinecker, J., 2000. Stress and deformation: Miocene to present-day tectonics in the Eastern Alps. *Tübinger Geowissenschaftliche Arbeiten (TGA) Reihe A*, 55, pp. 128.
- Reitner, J. M., van Husen, D., Finger, F., Linner, M., Krenmayer, H.G., Rupp, Ch., Egger, H., Schnabel, W., Bryda, G., Mandl, G.W., Nowotny, A., Pestal, G. and Schuster, R., 2006. *Geologische Karte von Oberösterreich 1:200 000*. Geologische Bundesanstalt, Wien.
- Robl, J. and Stüwe, K., 2005. Continental collision with finite indenter strength 1: Concept and model formulation. *Tectonics*, 24, TC4014, doi: 10.1029/2004 TC001727.

- Robl, J. and Stüwe, K., 2005. Continental collision with finite indenter strength 2: European Eastern Alps. *Tectonics*, 24, TC4014, doi: 10.1029/2004 TC001741.
- Robl J., Hergarten St. and Stüwe K., 2008a. Morphological analysis of the drainage system in the Eastern Alps. *Tectonophysics*, 460, 263–277.
- Robl J., Stüwe K., Hergarten S. and Evans L., 2008b. Extension during continental convergence in the Eastern Alps: The influence of orogen-scale strike-slip faults. *Geology*, 36, 963–966, doi 10.1130/G25294A.1
- Sachsenhofer, R.F., 1988. Zur Inkohlung des Ennstalertiärs. *Sitzungsberichte Österreichische Akademie der Wissenschaften, Mathematisch-Naturwissenschaftliche Klasse Abteilung I*, 197, 333–342.
- Sachsenhofer, R.F., Kogler, A., Polesny, H., Strauss, P. and Wagreich, M., 2000. The Neogene Fohnsdorf Basin: basin formation and basin inversion during lateral extrusion in the Eastern Alps. *International Journal of Earth Sciences*, 89, 415–430.
- Sachsenhofer, R.F., 2001. Syn- and post-collisional heat flow in the Cenozoic Eastern Alps. *International Journal of Earth Sciences*, 90, 579–592.
- Spang, J.H., 1974. Numerical dynamic analysis of calcite twin lamellae in the Greenport Center Syncline. *American Journal of Science*, 274, 1044–1058.
- Steininger, F.F., Rögl, F., Hochuli, P. and Müller, C., 1989. Lignite deposition and marine cycles. The Austrian Tertiary lignite deposits. A case history. *Österreichische Akademie der Wissenschaften, Sitzungsberichte der mathematisch-naturwissenschaftlichen Klasse Abteilung 1*, 197, 309–332.
- Strauss, P., Wagreich, M., Decker, K. and Sachsenhofer, R.F., 2001. Tectonics and sedimentation in the Fohnsdorf-Seckau Basin (Miocene, Austria): From a pull-apart basin to a half-graben. *International Journal of Earth Sciences*, 90, 549–559.
- Stur, D., 1853. Die geologische Beschaffenheit des Enns-Thales. *Jahrbuch der Geologischen Reichsanstalt*, 4, 461–483.
- Tollmann, A. und Kristan-Tollmann, E., 1963. Das Alter des hochgelegenen „Ennstal-Tertiärs“. *Mitteilungen der Österreichischen Geologischen Gesellschaft*, 104, 337–347.
- TRANSALP Working Group, Gebrande, H., Lüschen, E., Bopp, M., Bleibinhaus, F., Lammerer B., Oncken, O., Stiller, M., Kummerow, J., Kind, R., Millahn, K., Grassl, H., Neubauer, F., Bertelli, L., Borrini, D., Fantoni, R., Pessina, C., Sella, M., Castellarin, A., Nicolich, R., Mazzotti, A. and Bernabini, M., 2002. First deep seismic reflection images of the Eastern Alps reveal giant crustal wedges and transcrustal ramps. *Geophysical Research Letters*, 29/10, 92-1–92-4.
- Twiss, R.J. and Unruh, J.R., 1998. Analysis of fault slip inversions: Do they constrain stress or strain rate? *Journal of Geophysical Research*, 103, 12,205–12,222.
- Wagreich, M., Zetter, R., Bryda, G. and Peresson, H., 1997. Das Tertiär von Hieflau (Steiermark): Untermiozäne Sedimentation in den östlichen Kalkalpen. *Zentralblatt für Geologie und Paläontologie Teil I*, 1996, 633–645.
- Wagreich, M., Strauss, P.E., 2005. Source area and tectonic control on alluvial fan development in the Miocene Fohnsdorf intramontane basin, Austria. In: Harvey, A.M., Mather, A.E. and Stokes, M. (Eds.): *Alluvial Fans: Geomorphology, Sedimentology, Dynamics*. Geological Society, [London] Special Publications, 251, 207–216.
- Wang, X. and Neubauer, F., 1998. Orogen-parallel strike-slip faults bordering metamorphic core complexes: the Salzach-Enns fault zone in the Eastern Alps, Austria. *Journal of Structural Geology*, 20, 799–818.
- Weber, L. and Weiss, A., 1983. Bergbaugeschichte und Geologie der österreichischen Braunkohlenvorkommen. *Archiv für Lagerstättenforschung der Geologischen Bundesanstalt (Wien)*, 4, 140–144.
- Winkler-Hermaden, A., 1928. Über Studien in den inneralpinen Tertiärablagerungen und über deren Beziehungen zu den Augensteinfeldern der Nordalpen. *Österreichischen Akademie der Wissenschaften Sitzungsberichte mathematisch-naturwissenschaftliche Klasse Abteilung 1*, 137, 183–225.
- Winkler-Hermaden, A., 1951. Die tertiären Ablagerungen der Ennstalzone. In: *Schaffers Geologie von Österreich*, Wien, 415–422.
- Wölfler, A., Kurz, W., Fritz, H. and Stüwe, K., 2011. Lateral extrusion in the Eastern Alps revisited: refining the model by thermochronological, sedimentary and seismic data. *Tectonics*. (in press).
- Zentralanstalt für Meteorologie und Geodynamik Wien 2010. Regionalstelle Steiermark 2005.

Received: 10 March 2011

Accepted: 13 May 2011

Melanie KEIL¹ & Franz NEUBAUER

Dept. Geography and Geology, University of Salzburg, Hellbrunner Straße 34, A-5020 Salzburg, Austria;

¹ Corresponding author, melanie.keil2@sbg.ac.at

APPENDIX

TABLE 1

	Wörschach Wörschach Oberlengdorf		
	I	II	III
hornstein/chert		0.8	
Gutenstein Limestone			2.5
grayish limestone		5.1	
green quartzitic	1.6	0.8	
brown sandstone		0.8	1.7
yellow-brown sandstone			16.7
violet sandstone	0.8		
red sandstone		8.5	0.8
grayish sandstone		3.4	
Werfen Sandstone	1.7		
vein quartz	34.2	34.7	20.8
green schist		3.4	
reddish schist			0.8
lydite/black quartzite	25.0	11.9	8.3
gray phyllite			4.2
dark phyllite			5.0
green quartzitic phyllite			17.5
quartzitic schist	20.8	14.4	0.8
green quartzite			7.5
white marble	1.7	0.8	
serpentinite		5.1	0.8
orthogneis	13.3	10.2	12.5
amphibolite	0.8		
	100.0	100.0	100.0

TABLE 1: Details of provenance analysis of conglomerates of the Miocene Enns Valley basin fill in percentage.

A list of stations is given in Table 2. In many outcrops, superimposed sets of slickensides and striations indicate a poly-phase reactivation of these faults. However, some uncertainties of relative chronology remain. The determination of the succession of faulting and of displacement followed criteria proposed by, e.g., Petit (1987) and Gamond (1983, 1987). Paleostress orientation patterns were evaluated from this fault and slickenside data using numerical and graphical inversion methods proposed by Angelier and Méchler (1977), Angelier (1979, 1989), Armijo et al. (1982) and Marret and Almendinger (1990). These inversion methods indicate strain rather than paleostress patterns with relative magnitudes of principal stress axes (Twiss and Unruh, 1998).

Two numerical methods for calculating paleostress tensors were used in this work: NDA (Numerical Dynamic Analysis; Spang 1974) and direct inversion (Angelier 1979). The NDA method calculates the orientation of the principal axes of the paleostress tensor from summation of individual tensors for every plane. The direct inversion method minimizes the angles between the calculated directions of maximum shear stress

acting along the fault plane and the measured striae, which leads to the determination of the reduced stress tensor defined by the orientation of the principal stress axes and the stress ratio (Ortner et al. 2002). The quality of the calculation is checked in the normalized Mohr circle plot for three dimensional stresses. The age of each measured rock together with the principal orientation for each phase of deformation is given in Table 2.

Diagram	Tensor group	Method	λ1	λ2	λ3	R
1a	C	NDA	058/11	312/55	156/33	0.38
1b	A	NDA	156/18	256/28	037/56	0.35
1c	A	NDA	003/46	259/13	158/41	0.51
2a)	B	NDA	035/19	263/51	139/24	0.36
2b)	A	NDA	184/31	286/19	043/53	0.50
2c)	C	NDA	282/31	067/53	181/17	0.29
3a)	C	NDA	286/05	135/85	016/03	0.52
3b)	D	NDA	057/70	245/20	154/03	0.18
4	A	PT	309/28	131/69	046/14	
5	C	NDA	257/48	107/38	004/15	0.66
6	B	PT	015/32	119/13	197/66	
7a)	A	NDA	191/07	291/55	096/34	0.35
7b)	C	NDA	277/26	097/64	007/00	0.56
7c)	D	NDA	330/67	151/23	061/01	0.61
8a)	x	NDA	121/23	329/65	216/10	0.58
8b)	B	PT	213/00	292/64	129/14	
9a)	C	NDA	268/27	005/14	119/59	0.57
9b)	D	NDA	350/67	139/20	233/11	0.12

Site	Longitude	Latitude	Altitude	Lithology
1 Stoderzinken road	E 13°49'227	N 47°27'173	1670 m a.s.l.	Wetterstein Limestone
2 Stoderzinken road	E 13°49'226	N 47°27'138	1600 m a.s.l.	Wetterstein Dolomite S-side Wetterstein Limestone N-side
3 Stoderzinken road	E 13°49'066	N 47°26'587	1500 m a.s.l.	dolomite
4 Stoderzinken road	E 13°50'213	N 47°27'041	1205 m a.s.l.	dolomite
5 Stoderzinken road	E 13°50'331	N 47°26'568	1100 m a.s.l.	dolomite
6 Stoderzinken road	E 13°51'055	N 47°26'546	1048 m a.s.l.	Gutenstein Limestone
7 Quarry Winkl	E 13°51'341	N 47°27'554	929 m a.s.l.	massive limestone Wetterstein Dolomite
8 Untergrimming	E 14°03'358	N 47°31'388	681 m a.s.l.	Dachstein limestone
9 Wörschach	E 14°08'571	N 47°33'316	720 m a.s.l.	Gosau Conglomerate

TABLE 2: Structural analyses - description of sites; diagrams refer to Figure 10.